Original Research Article

Preliminary Research For Enabling Intelligent Focus For 3D Imaging

.

ABSTRACT

This research was basically on assessing the focus levels of images from tin ball samples as an ideal test. The results and method used for the ideal test sample was then applied to real datasets of samples like the canine kidney cells that have been infected with influenza virus for 24 hours. The samples of the tin ball samples and the influenza virus was viewed by the Dual Focused Ion Beam/ Scanning Electron Microscope (FIB/SEM). The FIB/SEM facility generated images of these samples. The analysis of these images was carried out by measuring Sharpness Function in images called the Derivative Sharpness Function using a software (Digital Micrograph); first on tin ball samples: which provided perfect results when a pixel difference of 1 was utilized but not so perfect result at a pixel difference of 20. Equally, a defocus increment of 0.01mm gave a perfect result better compared to a defocus image at 0.001mm displacement. Applying parameters from the successful result of the test samples on real data sets at 0.01mm and a pixel difference of 1 & 10 also produced reasonable results on assessing the levels of focus in real data samples such as the canine kidney cells.

Keywords: scanning electron microscope, Digital Micrograph, Derivative Sharpness Function, canine kidney cells.

1. INTRODUCTION

The aim of this research is to enhance the process of serial sectioning over long periods of taking images of datasets of samples by providing a method that could be the basis of automatic focus adjustment for the SEM/FIB. An SEM is a microscope that uses electrons instead of light to produce images. Serial sectioning is simply a process of dissecting a material into thin slices by a Focused Ion Beam , necessary for the SEM to take digital images of every slice therefore giving detailed information about the interior of the material. The materials used in this experiment were tin ball(ideal test) samples and real samples called the canine kidney cells. The kidney cells were stained using Uranium and Osmium based staining agents and encapsulated in epoxy resin. However, the samples do not remain in focus during these long runs serial sectioning on FIB; they tend to drift away from focus and sometimes even get destroyed. Before creating an intelligent technique necessary for creating an automatic focus adjustment of the images that drift out of focus, it is imperative to measure the levels of focus of the images produced during this process which is the primary objective of this research.

When a sample is placed in a FIB/SEM, a number of images are generated after several hours (depending on the operators desire). After sometime of serial sectioning producing images, the quality of the images later obtained is largely reduced: astigmatism is noted and the images are seen not to be in focus as well. This can hinder the process of generating the 3D reconstruction of the 2D images. To obtain microstructure parameters of some materials such as Li-ion cell samples, a 3D reconstruction of the several 2D images generated from the FIB/SEM is required using image processing softwares such as Avizo [1],[2]. Since at least, 50 2D images are needed to get reasonable information from the microstructure parameters about the material, the quality of the 2D images is also very important, hence the need to find an automated process for enhancing the quality of the 2D images is imperative.

2. MATERIAL AND METHODS

This section discusses the method used in obtaining images from tin ball samples and the canine kidney cells from the dual FIB/SEM, as well as the software (Digital Micrograph) utilized in processing the images and the method used in analysing the images in the Digital Micrograph.

2.1 Focused Ion Beam/Scanning Electron Microscope

The Focused Ion Beam in a FIB/SEM dual system slices the samples of the tin balls and canine kidney cells into thin samples for the Scanning Electron Microscope to take images [3],[4]. This is necessary because electrons have low penetration depth; therefore, thin samples are needed for the SEM to provide highly resolved spatial details of these samples. The dual FIB/SEM system was at *5.0 kV* and 0.40 nA during serial sectioning and with a magnification value of 5000*X* for tin ball samples. By adjusting the focus knobs on the SEM, defocused images were gotten. A schematic diagram of the dual FIB/SEM is shown in Figure 1.

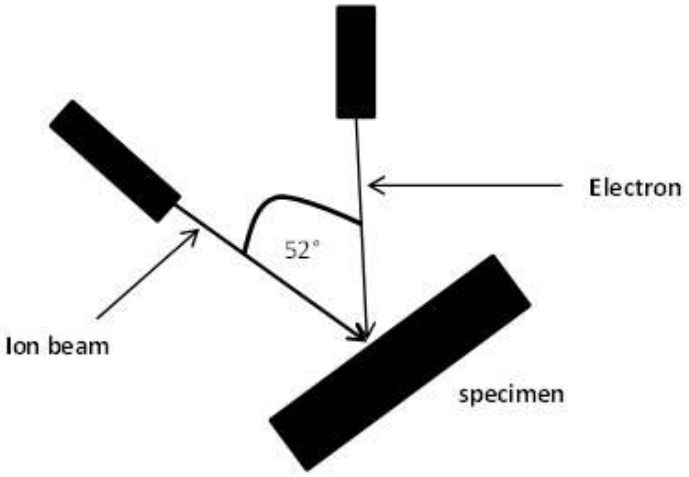

Figure 1 | A schematic diagram of the dual FIB/SEM. The angle between the FIB and SEM beams is 52º, with the ion beam at 90° to the specimen

By defocusing, we were simply adjusting the focusing lens and consequently expanding the size of the spot that is scanned across the sample, therefore features in the image became less sharply resolved. At 0 *mm* the image was in focus and millimetres away from zero, the images were in defocus. For focus and defocus datasets of images were obtained, with the first run having a defocus increment of 0.01 *mm*, the second, third and fourth run had 0.01 *mm,* 0.005 *mm* and 0.001 *mm* respectively. The experimental set up for the biological samples(canine kidney cells) was operated at the same condition(Voltage and Current) for the tin ball samples, but the magnifications were different i.e. the same set of biological samples in two different magnification values: 7500X three times at different defocus levels and 15000X, five times for different defocus levels. The defocus values for the former magnification values are:

0.01 *mm,* 0.005 *mm* and 0.001 *mm.* For the latter magnification, the defocus values were: 0.01 *mm,*0.005 *mm,*0.001 *mm,* 0.001 *mm and* 0.005 *mm*. The experiment was repeated to ensure all the defocus values used were exactly the same with that for the tin ball samples, hence, the repeated defocus values.

Fig. 2a, shows an image in focus, while Fig. 2b, 2c and 2d depict SEM images that are 0.01*mm*, 0.*02mm* and 0.03*mm out* of focus respectively.

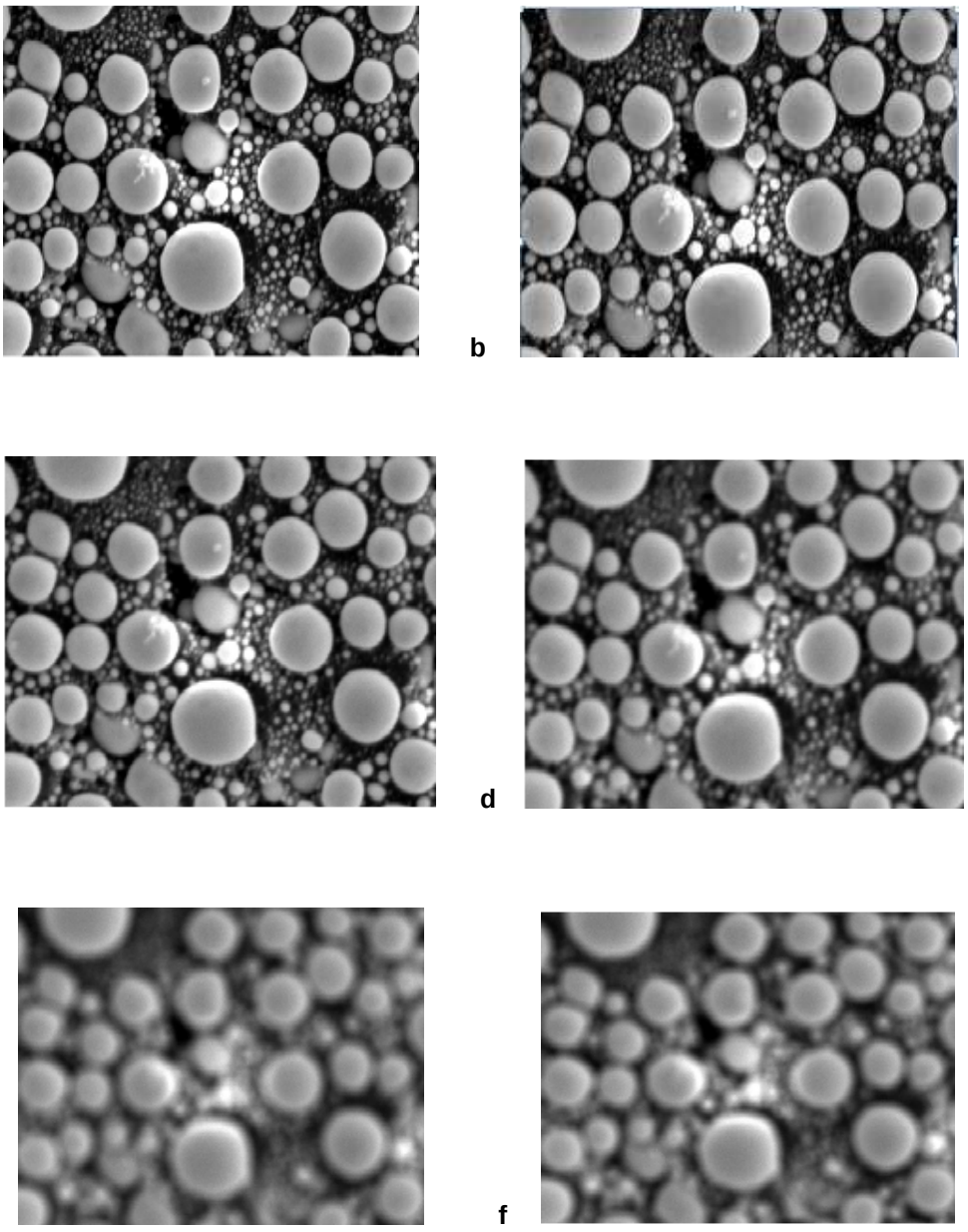

Figure 2 | SEM images of tin ball samples at different focus and defocus modes. (a) in focus 0.00mm**(b)** defocus 0.01mm **(c)** defocus 0.02mm **(d)** defocus value 0.03mm **(e)** defocus value 0.06mm **(f)** defocus value 0.07mm.

Looking at the images above, it is observed that the image in Fig. 2a is sharp and has no streak or blur. As seen from figure 2b to 2d the blurriness increases. This is due to increment in defocus values. The images in Figure 2(e) and 2(f) further illustrates the defocus concept using some of the pictures of the images. The images in Figures 2(e) and 2(f), further show that as the defocus value increases, so does the blurriness in the images increase.

2.2. DIGITAL MICROGRAPH

The Digital Micrograph is an image acquisition and processing software that provides SEM and Transmission Electron Microscope (TEM) users a complete package to also analyze and present image

and spectrum data. The functionality of a Digital Micrograph enables image processing tasks of all sorts to be accomplished using the powerful built-in C++ like script [5]. The software was extensively used in this project to process the data sets of images collected from the FIB/SEM. We started by using this software to calibrate each of the focus/defocus images which were originally 884 by 884 pixels to 1024 by 884 pixels. Fourier Transforms of each of the images was also gotten using this software. Written scripts were used to determine the Derivative Sharpness Function of defocus/focus datasets of images.

The process of finding the value of the derivative of a function is known as numerical differentiation. The derivative of a function represents the infinitesimal change with respect to one of its variables [6], which are the pixels of each of the images in this research. Sharpness Function is a real-valued estimation of discrete image sharpness. There are several methods used in deriving the Sharpness Function of an image. They are: the Derivative based Sharpness Function, Fourier transform based sharpness function, statistical based sharpness function. Among the different ways of evaluating sharpness function of images, it was investigated that the derivative based sharpness function and the Fourier transform based sharpness function were the best methods in evaluating this function. The derivative sharpness function, measures the intensity differences between neighbouring pixels of a defocus image. The mathematical equation for the DSF is shown below:

$$DSF = \Sigma_{i,j}\left|f_{i,j} - f_{i,j+k}\right|^{p} \text{ where } p\epsilon\{1,2\},\ i,j = 1024{,}884\ \&\ k\ is\ the\ pixel\ difference.$$

where f is a function of the pixel values in the vertical , (i) and horizontal, (j) axes of the images. p is known as the Brenner function. $p = 1$ was used to carry out the experiments.

Only the pixel difference taken in the horizontal distance is taken into account due to the fact that SEM scan is done only in the horizontal direction. DSF shows the effects of defocus by varying the pixel parameter in an axis. The images of the tin ball samples were originally $f_{1024,884}$. The displacement of the image became $f_{1024+k,884}$. The k values used in this experiment were 1,10,20 and 50. When $f_{1024+k,884}$ is subtracted from $f_{1024,884}$, the intensity difference between each of the neighboring pixels is obtained which is smaller in defocused images. The summation of the intensity differences gives the value of the DSF. The difference between pixels in an image is maximum when in focus.

3. RESULTS AND DISCUSSION

The method of DSF using the Digital Micrograph software was used to process the images one at a time and the corresponding derived images from the processed images are depicted in Figure 3. The images were first displaced at a pixel difference of 1 on the x-axis to give$1025\ against\ 884$. The displaced images were subtracted from the original ones and then summed up to give DSF images with their corresponding values.

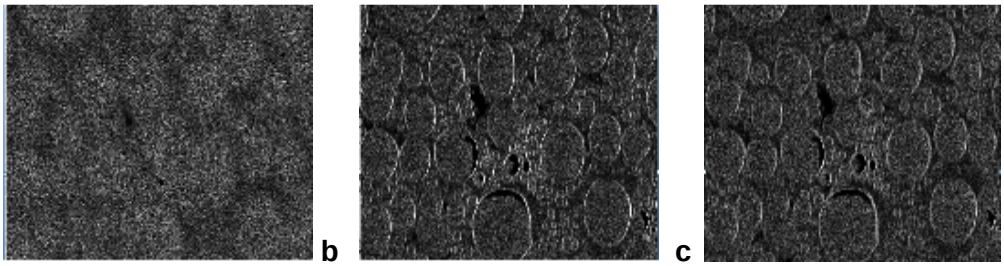

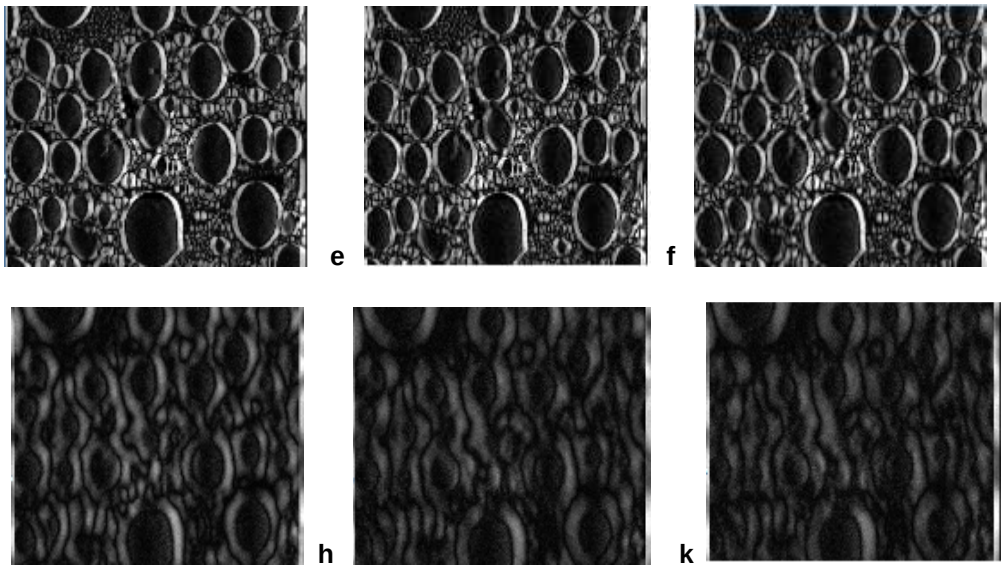

Figure 3 | Resulting images from the Digital Micrograph after processing using the Derivative Sharpness Function script. (a) 0.00mm**(b)** 0.01mm **(c)** 0.02mm. **At a pixel difference of 20 | (d)** 0.00mm **(e)** 0.01mm **(f)** 0.02mm **(g)** 0.08mm **(h)** 0.09mm **(k)** 0.10mm

Figure 3a is the DSF of an in-focus image of the tin ball samples, Fig. 3b is the DSF image $0.01mm$ out of focus. Fig. 3c, shows the DSF image $0.02mm$. The images of Fig. 3b and 3c traces of the tin ball samples while the DSF image in-focus does not. This is probably because the pixel difference of the defocused images is small i.e. 1. Carrying out the same method at a pixel difference of 20, shows a different perspective about the DSF.

Figure 3d shows the DSF of an in-focus image, while Fig. 3e and f show the DSF of images that are out of focus. Compared to the images in Fig. 3a, b and c, dark representation of the tin ball samples is shown even at when in-focus. Taking the DSF of defocused image of higher values to illustrate more on this experiment was imperative**.**

The DSF images as shown in Figures 3 g, h and k are defocused images of values $0.08mm, 0.09mm$ & $0.10mm$. They are not as bright as the DSF images in Figures $3d, e$ & f. This may be due to the low intensity differences in these highly defocused images. The value of the DSF is smaller in these images.

Using MATLAB [7], graphs of values of the DSF against the defocus increment were plotted as shown in the next page of the report. The reason for picking this *k* values was just to evaluate if a better result will be obtained at a higher *k* value than a lower value.

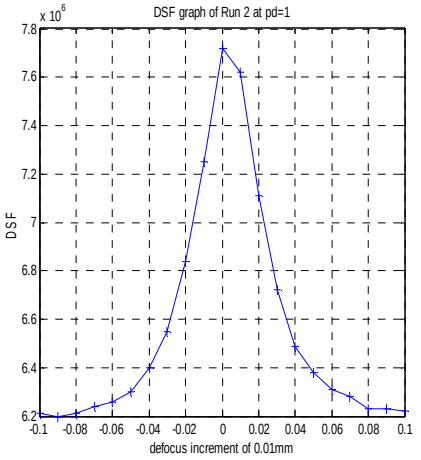

a

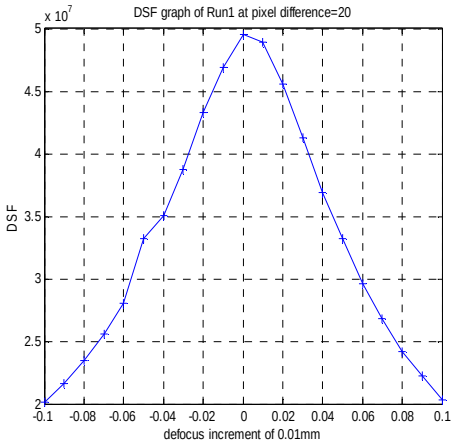

b

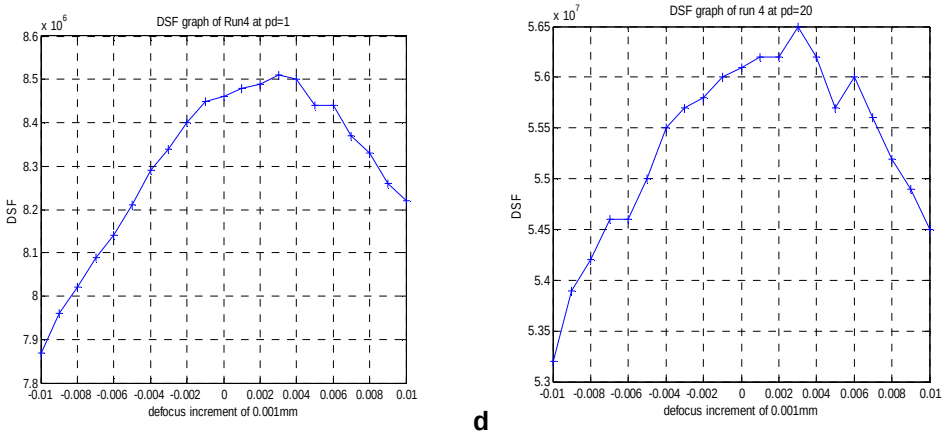

c d

Figure 4 | Plot of DSF values against defocus increment 0.01mm for (a) pixel difference (k) of 1 **(b)** pixel difference (k) of 20. **Defocus increment 0.001mm (c)** pixel difference of 1 **(d)** pixel difference(k) of 20.

Figure 4 a & b show graphs of the various DSF values against their respective defocus values. At a pixel difference of 1, as shown in Figure 4a the graph is more strongly peaked at the in-focus value 0*mm.* Both graphs have higher DSF values when in-focus than when they are out of focus. The DSF values against the defocus increment at a pixel difference of 20 are slightly evenly distributed compared to the pixel difference of 1 which have DSF values below 6.4 in the range $0.04mm - 0.10mm$ and $-0.04mm\ to - 0.10mm$ too. This showed that the DSF method showed better results at 20 pixel differences.

It was imperative to test the outcome of the results obtained when at the same pixel differences as the previous sub-section results have shown. In this experiment, a small value of defocus increment is worked on. The values of the DSF were plotted against an arithmetic series of 0.001*mm* respective defocus increment values as shown in the graphs.

The graphs of defocus series 0.01*mm* and 0.001*mm* at pixel differences of 1 & 20 are similar because of the peak defocus values the two of them have. In the DSF graphs of 0.001*mm,* the graphs are not strongly peaked at the 0.00 *mm*(in-focus) but at 0.003 *mm.* The DSF values in the 0.01 *mm* defocus values are not evenly distributed compared to the DSF graphs of 0.01*mm* shown in Figures 4a &b. Figure 4b graph is more strongly peaked at 0.003 *mm*, which indicates better results when *k* is > 1. Furthermore, comparing the results showed finding the Derivative Sharpness Function at a defocus value of 0.01 *mm* produces important results compared to smaller defocus values of $0.001mm$, that is, the DSF values with respect to their individual defocus values are evenly distributed and can provide useful information about defocus/focus levels of images.

As analyzed in the sections above to acquire useful, practical results about when best the Derivative Sharpness Function is ideal and best fit to measure the levels of focus/ defocus intensities in images, we then look at the possibility of applying the best fitted method on the canine kidney cells(biological cells). Below are sample images of the kidney cells:

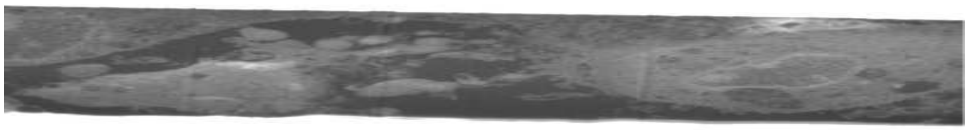

(a)

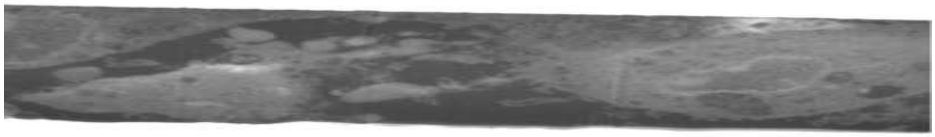

(b)

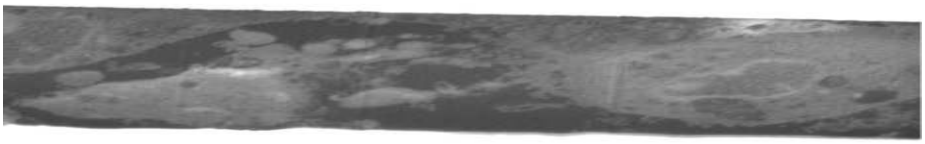

(c)

Figure 5 | SEM images of canine kidney cells. (a) in focus (0.00mm) **(b)** out of focus (0.05mm) **(c)** out of focus (-0.05mm)

Figures 5 a, b &c, are SEM images of the sample in cross-section after a trench has been opened and the face polished by the FIB. The image in Figure 5a was in focus while the images of Figure 5 b & c were out of focus. The images had the same number of pixels($1024\ by\ 884$) as the tin ball samples and there was no need for calibration: scanning of images by the SEM on these samples were applied in the horizontal direction, a different approach was utilized in deriving the Derivative Sharpness Function for each of the images. The pixel difference was added on the horizontal axis and not in the vertical axis as equally carried out in the tin ball sample experiment. This was because of the position in which the canine kidney cells were placed in the SEM. To find the DSF, images were replicated and then displaced by a pixel difference of 1 & 10 in the horizontal axis to give images having (1024,885) pixels and (1024,894) pixels respectively. These new images were then subtracted from the original image and the summation of the result of the pixels was derived.

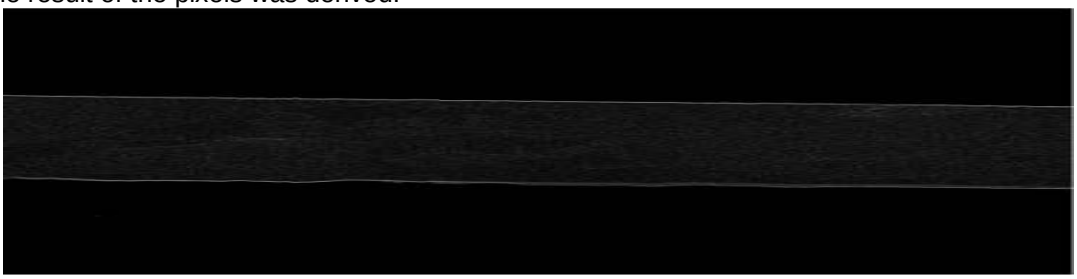

(a)

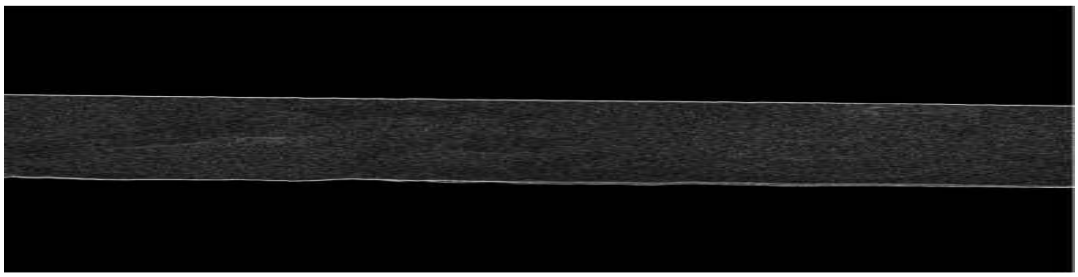

(b)

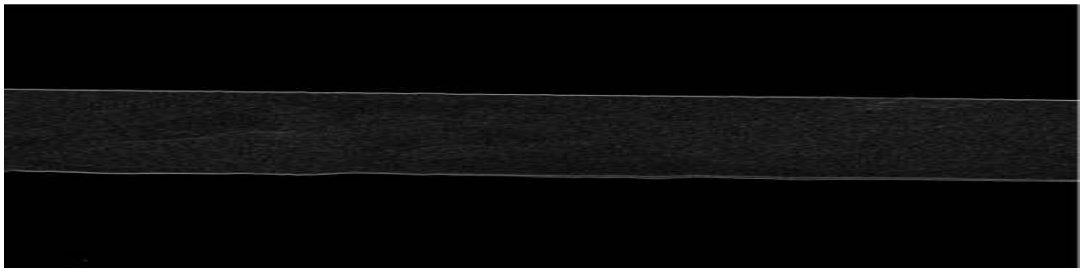

(c)

Figure 6 | DSF images of the canine kidney cells at (a) in focus (0.00mm) **(b)** out of focus (0.05mm) **(c)** out of focus (-0.05mm)

The DSF images of all the samples do not give reasonable resolved details of the cell as shown in images in Figure 6 a, b & c above. This is basically due to the original size of cells compared to tin ball samples. They are much smaller, therefore finding the DSF reduces the effect of using our natural eyes to see the details. Despite this, the values of the DSF gave some useful results as shown in the graphs in the next section.

Using MATLAB again, to plot graphs, the DSF results against each of its individual defocus value is depicted in Figure 7

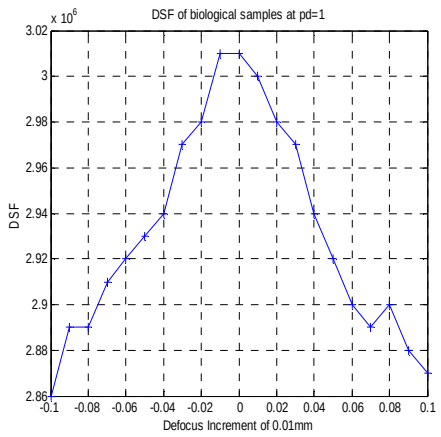

a

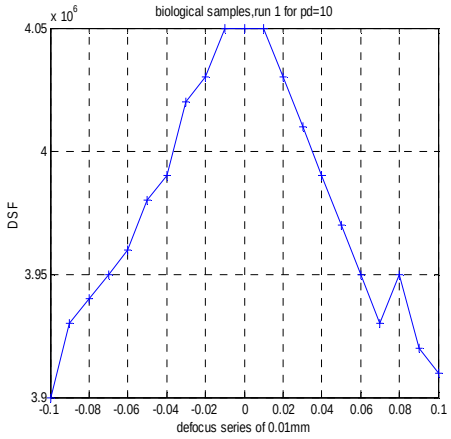

b

Figure 7 | Plot of DSF values against defocus increment 0.01mm for (a) pixel difference (k) of 1 **(b)** pixel difference (k) of 10

The graphs above show the DSF values against the defocus increment 0.01*mm* at pixel differences of 1 and 10 when the magnification was 7500X. The graph show a reasonable result similar to the result obtained in the graphs of figure 5a&b. Although at a pixel difference of 10 it shows the same values of DSF between focus and 0.01*mm* away from focus. The graphs are also strongly double-peaked which is not noticeable in the

results of the ideal tin ball samples.

4. CONCLUSION

The Derivative Sharpness Function against the defocus series of tin ball samples, which are ideal samples was shown to give results that are reasonable in measuring the focus/ defocus levels of images. When the best result was obtained at a defocus difference of 0.01 *mm*, this value was applied to real samples: the canine kidney cells. It showed a considerable measurement of the levels of focus/ defocus levels of images.

However, the DSF values obtained from a pixel difference of 1 when compared to a pixel difference of 10 and 20 were in values of hundreds, that it was quite difficult to use the program MATLAB to plot the DSF data obtained in these range on the same graph. Better results were obtained when the pixel difference is greater than 1. More research needs to be done in measuring levels of focus/defocus in images obtained from the FIB/SEM at pixel differences greater than 20. C++ codes that can be used in the FIB/SEM dual system needs to be written based on useful results obtained from this research and be ran on the system to reduce the level of drifts seen in images during the process of serial sectioning.

REFERENCES

1. Jochen, J. et al,Reconstruction of porous electrodes by FIB/SEM for detailed microstructure modelling. *Journal of Power Sources,* 2011:96

2. Jui-Ching Lin et al, Three-Dimensional Characterization of Pigment Dispersion Paint Films using Focused Ion Beam-Scanning Electron Microscopy. *Microscopy and Microanalysis,* 2012:18, 266-271.

3. McGrouther, D & Munroe, P.R. Imaging and Analysis of 3D Structure Using a Dual Beam FIB. *Microscopy Research and Technique,* 2007:70,186-194.

4. Gatan online. *Digital Micrograph*, 2012. Accessed:10 January,2014. Available from: http://www.gatan.com/imaging/dig_.php.

5. P.J. Grundy and G.A. Jones, *Electron Microscopy in the study of Materials*, Edward Arnold(publishers) limited, 1976.

6. Rudnaya, M.E. et al, Evaluating Sharpness Functions for automated scanning electron microscope. *Journal of Microscopy,*2010:240,38-39.

7. Wolfram Mathworld. *Derivatives*, 2014. Accessed: 10, January 2014. Available from:http://mathworld.wolfram.com/Derivative.html.